Research Advance

N-acetylation of α-synuclein enhances synaptic vesicle clustering mediated by α-synuclein and lysophosphatidylcholine

Chuchu Wang[1,2]#, Chunyu Zhao[1,2]#, Xiao Hu[3], Jiali Qiang[1,2], Zhenying Liu[1,2], Jinge Gu[1,2], Shengnan Zhang[1,2], Dan Li[4,5], Yaoyang Zhang[1], Jacqueline Burré[6], Jiajie Diao[3]*, and Cong Liu[1,7]*,

1. Interdisciplinary Research Center on Biology and Chemistry, Shanghai Institute of Organic Chemistry, Chinese Academy of Sciences, Shanghai 201210, China.

2. University of Chinese Academy of Sciences, Beijing 100049, China.

3. Department of Cancer Biology, University of Cincinnati College of Medicine, Cincinnati, OH 45267, USA.

4.Bio-X Institutes, Key Laboratory for the Genetics of Developmental and Neuropsychiatric Disorders (Ministry of Education), Shanghai Jiao Tong University, Shanghai 200030, China;

5. Zhangjiang Institute for Advanced Study, Shanghai Jiao Tong University, Shanghai 200240, China;

6. Brain and Mind Research Institute & Appel Institute for Alzheimer's Disease Research, Weill Cornell Medicine, New York, NY 10021, USA.

7. State Key Laboratory of Chemical Biology, Shanghai Institute of Organic Chemistry, Chinese Academy of Sciences, Shanghai, 200032, China

#These authors contributed equally to this work.

*To whom correspondence should be addressed. E-mails: jiajie.diao@uc.edu (J.D.) and liulab@sioc.ac.cn (C.L.)

Abstract

Post-translational modifications (PTMs) of α-synuclein (α-syn) such as acetylation and phosphorylation play important yet distinct roles in regulating α-syn conformation, membrane binding, and amyloid aggregation. However, how PTMs regulate α-syn function in presynaptic terminals remains unclear. Previously, we reported that α-syn clusters synaptic vesicles (SV)[1], and neutral phospholipid

lysophosphatidylcholine (LPC) can mediate this clustering[2]. Here, based on our previous findings, we further demonstrate that N-terminal acetylation, which occurs under physiological conditions and is irreversible in mammalian cells, significantly enhances the functional activity of α-syn in clustering SVs. Mechanistic studies reveal that this enhancement is caused by the N-acetylation-promoted insertion of α-syn's N-terminus and increased intermolecular interactions on the LPC-containing membrane. Our work demonstrates that N-acetylation fine-tunes α-syn–LPC interaction for mediating α-syn's function in SV clustering.

Keywords: N-acetylation, α-synuclein, vesicle clustering

Introduction

α-Syn is a highly abundant presynaptic protein in neurons. It is involved in synaptic vesicle (SV) clustering and the assembly of soluble N-ethylmaleimide sensitive factor receptor (SNARE) complex for mediating SV trafficking and neurotransmitter release[1,3,4]. Abnormal amyloid aggregation of α-syn and deposition into Lewy Bodies (LBs) is a pathological hallmark of Parkinson's disease[5-7]. Different types of post-translational modifications (PTMs), e.g. acetylation, ubiquitination, and phosphorylation have been identified to modify α-syn under physiological and pathological conditions[6,8-12]. Phosphorylation of S129 and Y39 is elevated, and this PTM-modified α-syn accumulates in LBs, implying a direct relationship between PTMs and α-syn pathology[9,10]. Rather than disease-related PTMs, additional PTMs e.g. N-acetylation and O-GlcNAcylation of α-syn were found also under normal conditions[13-15]. Specifically, N-acetylation can influence the conformation and increase the helicity of the N-terminal region of α-syn, alters its membrane-binding behavior, and is critical for oligomer formation and amyloid aggregation kinetics[16-18]. However, it remains unknown whether N-acetylation directly regulates the physiological function of α-syn in clustering SVs.

Results

N-terminal acetylation enhances SV clustering induced by α-syn.

In this study, we sought to investigate whether N-acetylation could modulate α-syn's function in promoting SV clustering. Firstly, we prepared recombinant N-terminally acetylated α-syn (Ac-α-syn) as well as unmodified α-syn (un-α-syn). N-terminal acetylation leads to a significant chemical shift perturbation of the first nine residues and H50 of α-syn in the solution nuclear magnetic resonance (NMR) spectrum (**Figure 1a, left**). Intriguingly, in-cell NMR experiments show that all of the un-α-syn is N-terminally acetylated once it is delivered into HEK-293T cells by electroporation (**Figure 1a, right**), which is consistent with a previous report[13]. This result confirms the physiological relevance of N-terminal acetylation of α-syn. Notably, N-terminal acetylation is believed to be irreversible in mammalian cells due to the lack of a known N-terminal deacetyltransferase. Hence, it is crucial to investigate the impact of N-acetylation on the function of α-syn. To further probe the influence of N-acetylation on α-syn-mediated SV clustering, we incubated mouse SVs with various α-synuclein variants (**Figure 1b, upper**). We next measured the extent of SV clustering by utilizing dynamic light scattering (DLS) to monitor alterations in particle diameters, as well as using negatively stained transmission electron microscopy (TEM) (**Figure 1b, middle and lower**). Notably, N-acetylation

significantly amplified α-syn's capacity to cluster SVs, which requires the N-terminal thirty residues (**Figure 1c-d**). These findings imply that N-acetylation augments SV clustering.

LPC mediates the enhancement of vesicle clustering by N-terminal acetylation of α-syn.

In our previous work, we found that α-syn can bind to both negatively charged dioleoyl-phosphoserine (DOPS)[1] and neutral lysophosphatidylcholine (LPC)[2]. Building on this, we sought to examine how N-acetylation affects SV clustering that arises from the interaction between α-syn and either of these lipids. To assess clustering functionality with specific lipid compositions, we synthesized liposomes mimicking SVs that contained either LPC or DOPS. We then used a single-vesicle clustering assay to track the clustering mediated by Ac-α-syn and un-α-syn (**Figure 2a**). Importantly, we observed that N-acetylation considerably boosted the clustering ability of α-syn with LPC-containing liposomes (**Figure 2b**). In contrast, N-acetylation did not increase the clustering of liposomes containing DOPS (**Figure 2c**). Therefore, LPC is responsible for the increased SV clustering activity by N-terminally acetylated α-syn.

N-terminal acetylation increases the α-syn–LPC interaction.

The interaction between α-syn and lipids is crucial for clustering SVs[1,2,19]. To elucidate the structural basis of how N-acetylation impacts the α-syn–LPC interaction, we carried out solution NMR titration analyses to examine the α-syn–LPC interaction with residue-specific resolution. Adding increasing concentrations of pure LPC micelles to unmodified α-syn resulted in a dose-dependent and continuous attenuation of signals for the first 100 residues of α-syn, indicating these residues can interact with LPC (**Figure 3a, upper**). Notably, N-acetylation significantly elevated the binding affinity of the N-terminal region (residues 1-30), particularly the initial 10 residues, towards LPC, leading to a rapid binding pattern during titration (**Figure 3a, lower**). Moreover, Ac-α-syn demonstrated a sequential binding behavior with LPC, where the N-terminal region (residues 1-30) bound initially, succeeded by the central region (residues 30-100) as the LPC/Ac-α-syn ratio increased (**Figure 3a, lower**). Similar trends were observed in NMR titrations using DOPC/LPC-mixed liposomes (**Figure 3b**). On the other hand, N-acetylation only slightly weakened the interaction between the N-terminal region (residues 1-30) and DOPS, particularly at low DOPS/α-syn ratios, resulting in a continuous signal attenuation for the first 100 residues (**Figure 3c**). These findings reveal that N-acetylation considerably enhances the N-terminal

region's binding affinity, particularly the first 10 residues, to LPC, while modestly reducing the same region's affinity to DOPS.

To provide insights that are more relevant to physiological conditions, we extended our investigation to examine how Ac-α-syn interacts with SV membranes. By utilizing a protocol established before[20], we prepared monodisperse SVs isolated from normal mouse brains and titrated them with Ac-α-syn at an SV/α-syn ratio of 260:3000, which is a physiologically relevant ratio within presynaptic terminals as determined in previous work[21]. The HSQC spectrum revealed signal attenuation, notably in the N-terminal region and specifically within the first 10 residues of α-syn (**Figure 3d**). These findings closely mirrored those observed when Ac-α-syn was titrated with LPC micelles and DOPC/LPC-mixed liposomes at low lipid/α-syn ratios of 10:1 and 100:1, respectively (**Figure 3e**). These results further substantiate the critical role played by the N-terminal region of Ac-α-syn in SV membrane binding.

Ac-α-syn binding on LPC shows high intermolecular interactions

The intermolecular interactions between α-syn monomers[19] or between α-syn and vesicle-associated membrane protein 2 (VAMP2)[1] are also essential for clustering SVs. To further characterize the accessibility of α-syn to LPC and DOPS, we performed cross-linking experiments coupled with mass spectrometry (XL-MS). We mixed ^{15}N-labeled and unlabeled Ac-α-syn at a 1:1 ratio and selected the cross-linked fragments containing both ^{15}N-labeled and unlabeled Ac-α-syn to map the intermolecular cross-linking pattern. We found the accessibility of α-syn to LPC to be much higher than that to DOPS (**Figure 4a**). The number of cross-linked peptide pairs, indicative of their close interaction, detected in LPC-induced multimers was over twice more than that of DOPS (**Table S1-6**). This result demonstrates high intermolecular interactions between Ac-α-syn and LPC.

Discussion

In summary, the interaction between α-syn and lipids plays a crucial role in both the protein's physiological functions in SV trafficking and its pathological aggregation, as observed in neurodegenerative conditions[22]. Understanding how PTMs like N-acetylation modulate these interactions and their subsequent effects is a critical area of study. Notably, in addition to in-cell NMR findings that demonstrate spontaneous acetylation of α-syn, N-acetylated α-syn has been observed in PD patients' brain tissue, underscoring its physiological relevance[23]. Our research reveals that N-acetylation

enhances the binding of the N-terminal region of α-syn to LPC, thereby facilitating its association with SVs. LPC is a neutral lipid with an inverted-cone shape, known to create high membrane curvature and more lipid packing defects[24]. N-acetylation effectively neutralizes the positive charge of α-syn's N-terminus, fostering its insertion into LPC-rich membranes through hydrophobic interactions. Conversely, N-acetylation significantly reduces the affinity of α-syn's N-terminal region for negatively charged PS-containing membranes, where the interaction is mainly electrostatic in nature. Furthermore, compared to DOPS, the interaction between N-terminally acetylated α-syn and LPC also triggers more intermolecular interactions that support the functional α-syn for SV clustering (**Figure 4b**).

Most recently, we reported that α-syn also interacts with the neutral phospholipid LPC, which could be enriched in synaptosomes. LPC can facilitate α-syn to perform its function on clustering SVs[2]. Meanwhile, a recent study showed that LPC can reduce α-syn aggregation[25], demonstrating the importance of the α-syn–LPC interaction. Since α-syn is N-terminally acetylated in mammalian cells, the involvement of LPC, not anionic phospholipids, in N-acetylation-enhanced SV clustering demonstrates the importance of our recently reported α-syn–LPC interaction for mediating α-syn's function in SV trafficking. Furthermore, the amount of anionic phospholipids on SVs could change with aging and disease[26], which may alter the binding modes of α-syn. The α-syn–LPC interaction enhanced by N-acetylation could serve as an alternative mechanism for maintaining the SV clustering function of α-syn.

Materials and Methods

Lipids. Lipids used in this study were purchased from Avanti Polar Lipids as follows: 16:0 LPC (1-palmitoyl-2-hydroxy-sn-glycero-3-phosphocholine) (855675), DOPC (1,2-dioleoyl-sn-glycero-3-phosphocholine) (850375), DOPS (1,2-dioleoyl-sn-glycero-3-phospho-L-serine) (840035), POPC (1-palmitoyl-2-oleoyl-glycero-3-phosphocholine) (850457), POPE (1-palmitoyl-2-oleoyl-sn-glycero-3-phosphoethanolamine) (850757), biotin-DPPE (1,2-dipalmitoyl-sn-glycero-3-phosphoethanolamine-N-(cap biotinyl)) (870277), cholesterol (70000).

Protein purification. N-terminal unmodified human α-syn (un-α-syn) and N-terminal 30-residue truncated α-syn (Δ30 α-syn) were cloned into the pET22 vector. For the N-terminal acetylated α-syn (Ac-α-syn), the fission yeast NatB complex (N-acetyltransferase) gene was co-expressed with α-syn in bacteria to acetylate its N-terminus [27]. ^{15}N isotope-labeled Ac-α-syn or α-syn were produced in M9 minimal medium with uniformly labeled $^{15}NH_4Cl$ (1 g/L, Cambridge Isotope Laboratories). Not isotope-labeled Ac-α-syn or α-syn were produced in the Luria-Bertani (LB) medium. Expression was induced by 1 mM isopropyl-1-thio-D-galactopyranoside (IPTG) at 37 °C in *E.coli* strain BL21-DE3, which OD_{600} reached 0.8-1.0. The collected bacteria were lysed in 100 mM Tris-HCl (pH 8.0), 1 mM EDTA, and 1 mM phenylmethylsulfonyl fluoride (PMSF). The lysates were boiled for 10 min followed by centrifugation at 16,000 g for 30 min. 20 mg/ml streptomycin was mixed with supernatants. After a 30-min centrifugation at 16,000 g, the pH value of supernatants was adjusted to 3.5 by 2 M HCl, followed by centrifugation at 16,000 g for 30 min. The supernatants were then dialyzed in 25 mM Tris-HCl (pH 8.0) overnight at 4 °C. The dialyzed protein solution was filtered through a 0.22 μm membrane (Merck Millipore, SLGP033RB) and injected onto an ion-exchange Q column (GE Healthcare, 17515601), followed by further purification via size exclusion chromatography (GE Healthcare, Superdex^{TM} 75).

Isolation of synaptic vesicles from mouse brains. Neuronal synaptic vesicles (SV) were isolated from 8-week-old C57BL6 male mice (Lingchang Shanghai) by following published protocols [28]. The experiment was performed at 4 °C or on ice with pre-cooled reagents. Four fresh brains (~0.5 g for each) were homogenized in 25 mL 4 mM HEPES-NaOH (pH 7.4) and 320 mM sucrose buffer (HB) with protease inhibitors by using a PTFE pestle in a 40 mL glass tube (Sigma, P7984). The homogenate was centrifuged at 1,500 g for 10 min. The supernatant (S1) was collected and kept on ice. The pellet was resuspended with 25 mL HB and homogenized, followed by centrifugation at 1,500 g for 10 min. Then the supernatant (S2) combined with S1 was centrifuged at 20,000 g for 20 min. The pellet which contains synaptosomes was resuspended with 2 mL HB and then homogenized in 20 mL H_2O followed by adding 50 μL of 1M HEPES-NaOH (pH 7.4) and protease inhibitors. The homogenate was placed on ice for 30 min, and centrifuged at 20,000 g for 20 min. The supernatant was ultra-centrifuged at 70,000 g for 45 min. The pellet was resuspended in buffers indicated in each analysis and homogenized by using a PTFE pestle in a 3 mL glass tube (Sigma, P7734). To further disrupt any remaining SV clusters before experiments, the homogenized SVs were drawn first through a 20-gauge hypodermic needle (Fisher Scientific, 0556121) attached to a 10-ml syringe, and then through a 27-gauge needle (Fisher Scientific, 22557176) and expelled. Mice experiments were conducted according to the protocols approved by the Animal Care Committee of the Interdisciplinary Research Center on Biology and Chemistry (IRCBC), Chinese Academy of Sciences (CAS).

α-Syn-mediated SV clustering monitored by dynamic light scattering (DLS). The DLS experiments were performed using a DynaPro Nanostar instrument (Wyatt Technology, Santa Barbara, CA). A 50 µL aliquot of each sample containing homogenous SV (total protein concentration of 50 µg/mL) and α-syn variants (3 µM) was used for DLS measurement. The buffer used in this assay was 50 mM HEPES-KOH (pH 7.4), 150 mM KCl. The following parameters were set for all measurements: correlation function low cutoff was 1.5 µs; correlation function high cutoff was 6×10^4 µs; peak radius low cutoff was 0.5 nm; peak radius high cutoff was 10^4 nm. The results were reported as the average of 10 consecutive autocorrelation functions (acquisition time = 5 s), and each sample was repeatedly measured three times.

Negatively stained transmission electron microscopy (TEM). An aliquot of 5 µL sample was pipetted onto a glow-discharged carbon-coated copper grid. 5 µL 3% (w/v) uranyl acetate was used for negative staining after washing the grid twice with 5 µL distilled H_2O. The grid was air-dried after removing extra uranyl acetate by filter paper. TEM images were obtained by an electron microscope (Thermo Fisher FEI Tecnai G2 TEM) at 120 kV equipped with a LaB_6 gun and a FEI BM Eagle CCD camera.

Liposome preparation. DOPS dissolved in chloroform was evaporated using a dry nitrogen stream. The dried lipid film was hydrated in buffers used for cross-linking (indicated below), and then sonicated in a water bath at 65 °C for 10 min. To mimic the size of synaptic vesicles, the hydrated lipids were extruded 41 times at 65 °C through a poly-carbonate film with a pore size of 50 nm (Whatman Nucleopore Track-Etch) by using an extruder apparatus (Avanti Polar Lipids, 610000). LPC powder was dissolved in buffers used for cross-linking for further analysis.

Single-vesicle clustering assay. The protein-free liposomes (~100 nm) of POPC, POPE, cholesterol, LPC or DOPS, and biotin-DPPE or DiD (Invitrogen, D307) were prepared in the single-vesicle clustering buffer (25 mM HEPES-NaOH (pH 7.4), 100 mM NaCl) to a total lipid concentration of ~10 mM. The group of unlabeled liposomes contains POPC, POPE, cholesterol, LPC or DOPS and biotin-DPPE with a molar ratio of (49.9~59.9):20:20:(0~10):0.1. The group of labeled liposomes contain POPC, POPE, cholesterol, LPC or DOPS and DiD with a molar ratio of (49~59):20:20:(0~10):1. LPC or DOPS on both vesicles was varied from 0 to 10%, in expense of POPC.

For the clustering experiments, the unlabeled liposomes (100 µM) were injected into the sample chamber and incubated for 30 min, followed by buffer exchange of 300 µL single-vesicle buffer. 10 µM DiD labeled liposomes were incubated with 20 nM α-syn or Ac-α-syn, and loaded into the sample chamber with 30 min incubation at room temperature. Unbound DiD liposomes and proteins were removed by buffer exchange of 300 µL single-vesicle buffer. Sample slides with multiple channels were monitored in a wide-field TIR fluorescence microscope. Data were acquired with a CCD camera, and analyzed with the smCamera program. Six images were taken at random locations within each channel on the quartz slide. The number of liposome interactions (clustering) was determined by counting the number of fluorescent spots from the emission of DiD upon excitation at 633 nm. Details were described previously [1,29].

Delivering ^{15}N-un-α-syn into mammalian cells by using electroporation method. Electroporation was performed with a Neon transfection system (Invitrogen, MPK5000). Lyophilized ^{15}N-un-α-syn was dissolved in Buffer R (Invitrogen, MPK10025) to a final concentration of 300 µM. HEK-293T cells (ATCC, CRL-3216) were collected and washed with PBS for 3 times to get rid of medium. Cells were

resuspended in ^{15}N-un-α-syn solution at 8×10^7 cells per mL. Eight aliquots of 100 μL cell-protein mixture were pipetted and electroporated. Pulse program was: 1,400 V pulse voltage, 20 ms pulse width, 1 pulse number. Electroporated cells were added into four 10 cm-diameter dishes with pre-warmed culture medium. Cells were allowed to recover for 5 h, and were then harvested by trypsinization and washed with PBS four time. Resuspended cells were washed in 160 μL pH-stable L-15 medium (Gibco, 11415064) and 40 μL D$_2$O, and allowed to settle in a 5 mm NMR tube by gentle sedimentation with a hand-driven centrifuge. The supernatant was discarded. Finally, ~500 μL sedimented cell slurry was prepared for NMR measurement.

In-cell and *in vitro* solution NMR spectroscopy. In-cell NMR experiments were carried out at 25 °C on a Bruker 900 MHz spectrometer equipped with a cryogenic probe by following a published paper [20]. Bruker standard SOFAST-HMQC pulse sequence [30,31] was used and the ^{1}H shape pulse efficient was optimized for collecting the 2D NMR spectrum of the in-cell samples with 80 scans. The delay time (D1) was set to 0.29 s, and 1024 and 128 complex points were used for ^{1}H and ^{15}N, respectively. The experiment duration time is 61 min 16 s. Cell viability before and after the SOFAST-HMQC NMR experiment was assessed by trypan blue staining. Cell viability remained above 90% after the NMR experiments.

In vitro NMR experiments were carried out at 25 °C on an 800 MHz Agilent spectrometer equipped with a cryogenic probe (Agilent Technologies). The buffer used in all NMR titration assays was 50 mM sodium phosphate buffer (pH 6.5) containing 50 mM NaCl and 10% D$_2$O (v/v). All of the LPC or liposomes were prepared with a total molar concentration of 50 mM, and gradually added to the 500 μL 50 μM N-acetylated or unmodified α-syn in a series of NMR titration assays. In NMR SV-titration experiment, each spectrum was acquired from separately prepared samples with increasing amounts of SV in 50 μM N-acetylated α-syn. The molar concentration of SVs was calculated according to parameters from a published paper [32].

All the NMR data were processed using NMRPipe and analyzed by SPARKY [33]. Backbone resonance assignment of N-acetylated and unmodified α-syn was accomplished according to a published paper [13] and a Biological Magnetic Resonance Bank (BMRB) entry 6968 [34], respectively.

α-Syn multimer cross-linking experiment
LPC micelles, DOPS liposomes, and α-syn variants were mixed in a cross-linking-buffer (10 mM HEPES-NaOH, pH 7.4). The stock of cross-linker disuccinimidyl suberate (DSS) (Thermo Scientific, 21658) was dissolved in DMSO to 40 mM. 50 μM protein and 2 mM DSS were incubated at indicated concentrations of lipid in the cross-linking-buffer at 25 □ for 1 h. Crosslinking was terminated by the addition of 100 mM Tris-HCl (pH 7.4) at 25 □ for 10 min. For identification of the inter-molecular cross-linked peptide pairs from α-syn multimers by MS analysis, the half amount of α-syn was ^{15}N-labeled α-syn.

Protein cross-linking mass spectrometry (XL-MS) analysis
The cross-linked samples were precipitated using acetone at −20 °C for 30 min. Precipitates were dried in air and resuspended in 8 M urea in 100 mM Tris-HCl (pH 8.5). Then, 5 mM TCEP was adding for 20 min incubation, followed by adding 10 mM iodoacetamide for 15 min for alkylation reaction in the dark. Then, the samples were diluted to 2 M urea in 100 mM Tris-HCl (pH 8.5), and digested with trypsin (molar ratio of protein to trypsin was 50:1) at 37 °C for 16 h in the presence of 1 mM CaCl$_2$ and 20 mM

methylamine. Digestion was terminated by adding formic acid to 5% final concentration (v/v). After desalting by C18 desalting tips, the digested samples were air-dried and stored at -80 ☐ until analysis.

The digested peptides were analyzed by online nanoflow liquid chromatography-tandem mass spectrometry (LC–MS/MS). Briefly, nano LC–MS/MS experiments were performed on an EASY-nLC 1000 system (Thermo Scientific) connected to an Orbitrap Q Exactive HF (Thermo Scientific) through a nanoelectrospray ion source. The peptides were separated on a nano-column (C18, 100 μm × 15 cm, 1.9 μm, 120 Å) and further analyzed using an Orbitrap Q Exactive HF mass spectrometer. A 60-min gradient was used in the nano LC at 300 nL/min flow rate: 0-4 min from 4% buffer B (80% ACN, 0.1% FA), 96% buffer A (0.1% FA in water) to 8% buffer B, 4-45 min from 8% buffer B to 22% buffer B, 45-53min from 22% buffer B to 30% buffer B, then increasing to 95% buffer B in the next 41min, and stay 95% buffer B for 3 min. One full-scan mass spectrum (350-1500 m/z) at a resolution of 60,000 followed by HCD fragmentation and detection of the fragment ions (scan range from 350 to 1,500 m/z) in Orbitrap at a 27% normalized collision energy was repeated continuously.

The cross-linked peptide pairs were identified by pLink[35] first. The pLink search parameters used in this study include: (1) 20 ppm for a window of precursor mass tolerance. (2) 4 ppm for a window of fragment mass tolerance. (3) Lys for cross-linking sites of the cross-linker DSS. (4) 138.0680796 Da for xlink mass shift. (5) 156.0786442 Da for monolink mass shift. (6) 57.02146 Da for fixed carbamidomethyl-Cys modification mass shift. (7) 15.99491 Da for variable Met modification mass shift. (8) 4-100 amino acids per chain for peptide length. (9) 400-10,000 Da per chain for peptide mass. (9) 2 missed cleavage sites per chain for trypsin digestion of protein. The searching results were filtered with a false rate of less than 5% and E-values of less than 0.0001.

The pLink readout data were filtered with a score less than 10^{-6} and mass error for crosslinking assignments less than 4 ppm. To identify the inter-protein cross-linked peptide pairs, the spectrum (ΔRT < 0.5 s) of the two cross-linked peptide segments needs to be manually checked with four peaks of ^{14}N-peptide and ^{14}N-peptide, ^{14}N-peptide and ^{15}N-peptide, ^{15}N-peptide and ^{14}N-peptide and ^{15}N-peptide and ^{15}N-peptide.

Author contributions: J.D., and C.L. designed and directed the study. C.W., C.Z., Z.L., J.G., and S.Z. prepared proteins, performed cellular and cross-linking experiments, and carried out EM, NMR, and MS measurements. X.H. performed single-vesicle experiments. D.L., Y.Z., J.B., J.D., and C.L. analyzed the data, discussed the results, and wrote the manuscript.

Competing interests: The authors declare no competing financial interests.
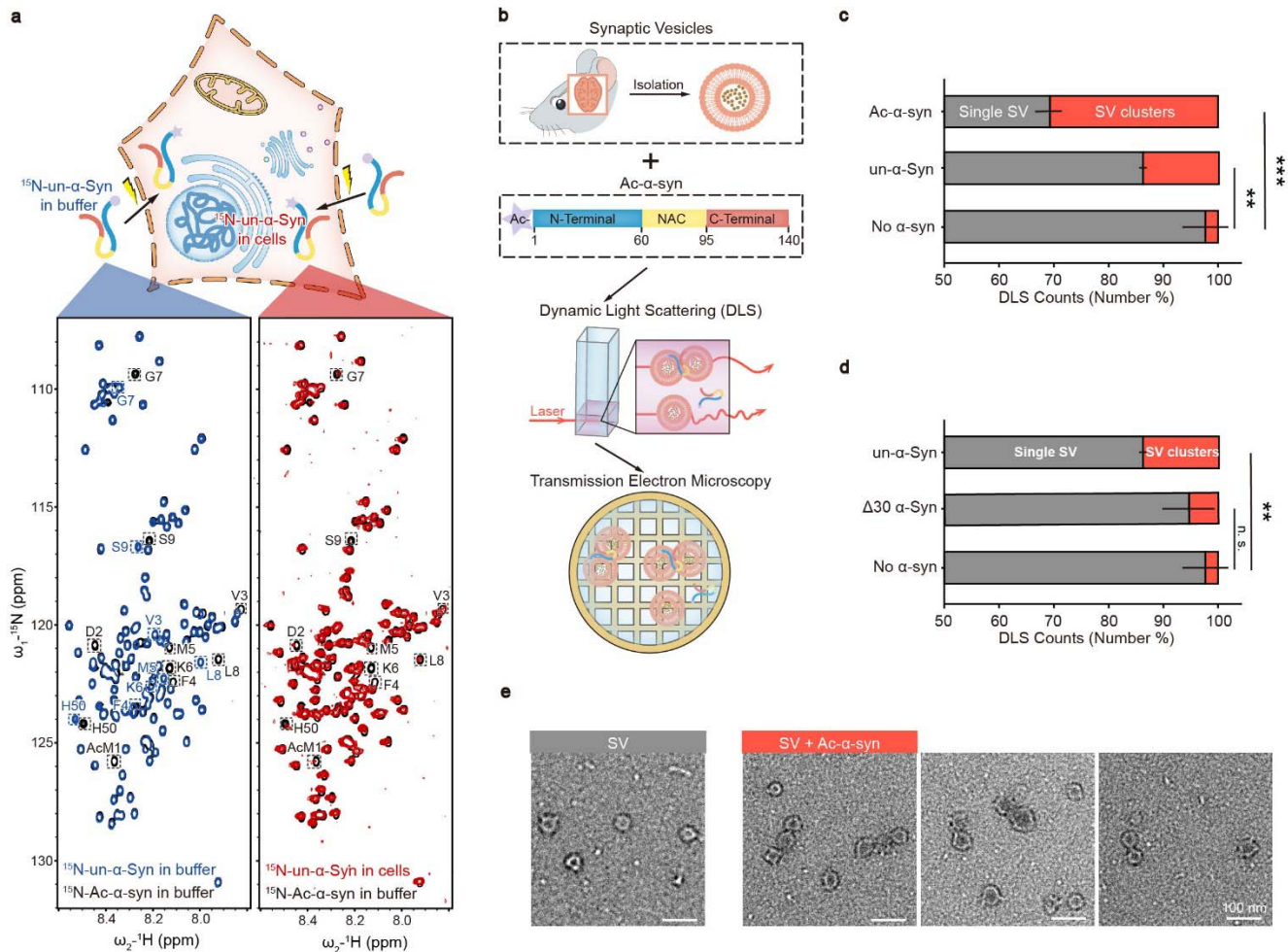
Figure 1 N-terminal acetylation enhances SV clustering induced by α-syn. (**a**) α-syn is N-terminally acetylated in cells. Upper: Schematic representation of the delivery of ^{15}N-labeled N-terminally unmodified α-synuclein (un-α-syn) into mammalian cells through electroporation. Lower: Comparisons of 2D ^{1}H-^{15}N HSQC spectra of N-acetylated α-syn (Ac-α-syn) (black) with in-buffer un-α-syn (blue) and in-cell un-α-syn (red). Distinct assignments for NMR cross-peaks corresponding to amino acids in Ac-α-syn and un-α-syn are enclosed and labeled. (**b**) Scheme of experimental design for the functional study of Ac-α-syn on SV clustering. SVs isolated from mouse brains were added to Ac-α-syn (Upper) for measuring size distribution by DLS (middle), and the sample was further visualized by using negatively stained TEM (lower). (**c**) The influences of N-acetylation of α-syn and (**d**) α-syn without the N-terminal thirty residues on SV clustering measured by DLS. The X-axis represents the number percent of the single SV and clustered SVs counted by DLS. Error bars are standard deviations from 3 biological replicates. **, p-value < 0.01; ***, p-value < 0.001; analysis by Student's t-test. (**e**) Representative negatively stained TEM images of the single SV and clustered SVs in SV samples with no α-syn (grey) and Ac-α-syn (red), respectively.
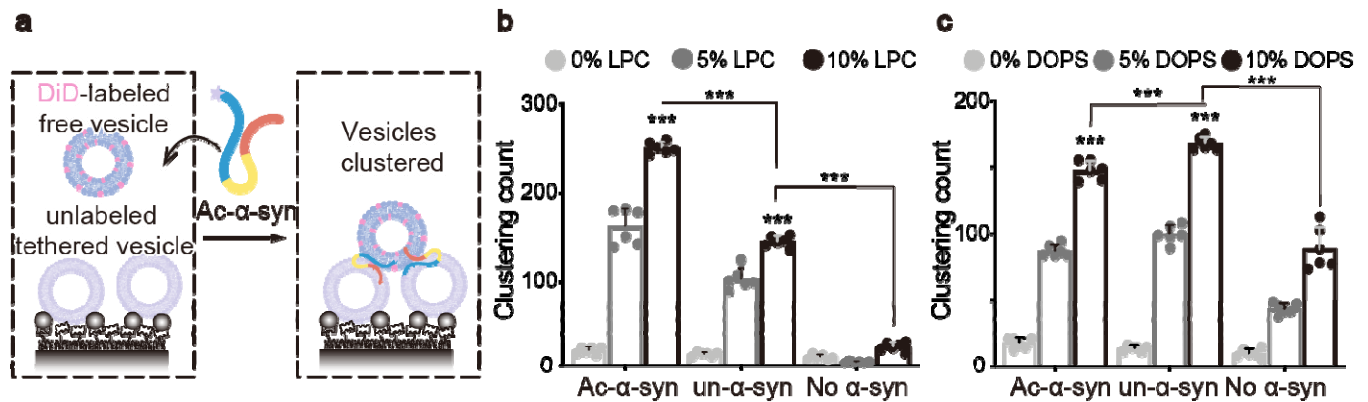
Figure 2 LPC mediates the enhancement of vesicle clustering by N-terminal acetylation of α-syn. (**a**) Scheme of single-vesicle clustering assay for the functional study of Ac-α-syn on vesicle clustering. Vesicles were prepared with different amounts of LPC, and labeled with DiD and unlabeled, respectively. A saturated layer of unlabeled vesicles was immobilized on the imaging surface. Free DiD-vesicles were injected into the system with Ac-α-syn. Red laser illumination imaged the DiD-vesicles that clustered with unlabeled vesicles. The enhancement of LPC (**b**) and DOPS (**c**) on single vesicle clustering count by Ac-α-syn and un-α-syn, respectively. Error bars are standard deviations from 6 random imaging locations in the same sample channel. *** indicates p-value < 0.001, analysis by Student's t-test.
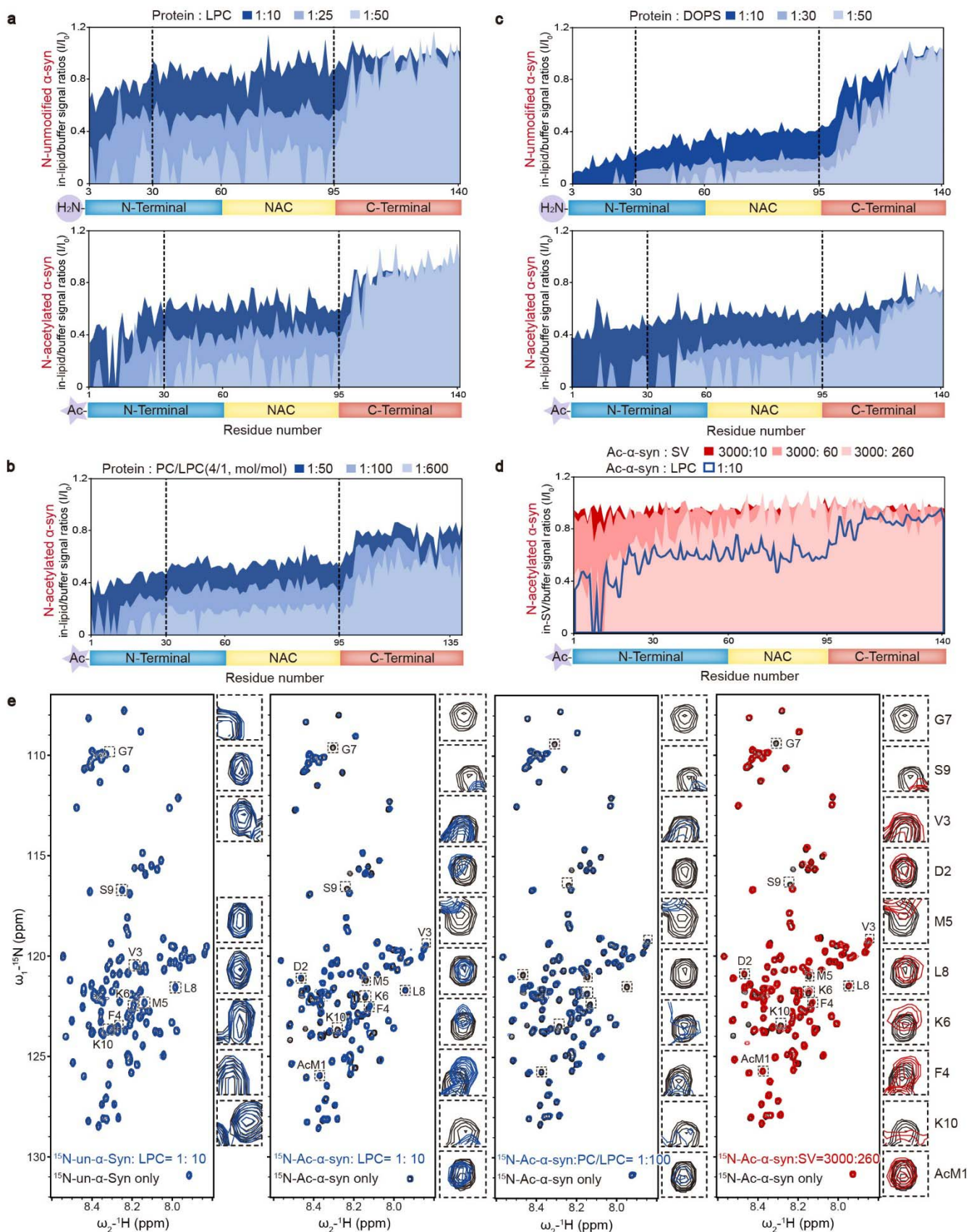
Figure 3 N-terminal acetylation increases the α-syn–LPC interaction. Comparisons of residue-resolved NMR signal intensity ratios (I/I_0) of un-α-syn (upper) and Ac-α-syn (lower) during titration with LPC micelles (**a**), LPC-containing liposomes (DOPC:LPC = 4:1, mol: mol) (**b**), and DOPS liposomes (**c**) at indicated protein/lipid molar ratios. Dash lines highlight the residue positions of 30 and 95. (**d**) SVs isolated from mouse brains were employed for NMR titration with ^{15}N-Ac-α-syn, approximating the physiological ratio (α-syn:SV = 4000:300, mol: mol). Residue-resolved NMR signal intensity ratios (I/I_0) of Ac-α-syn titrated by SVs to that in solution. The molar ratios of SV to Ac-α-syn are indicated. LPC titration in the Ac-α-syn/LPC ratio of 1:10 (blue curve) is overlaid on the SV titration. (**e**) 2D ^{1}H-^{15}N HSQC spectra of NMR for un-α-syn with LPC micelles and Ac-α-syn with LPC micelles, LPC-containing liposomes, and mouse SVs. The NMR cross-peaks of the first 10 residues are highlighted and magnified, as depicted on the right side of each spectrum set (Note: the first and second residues of un-α-syn cannot be assigned).
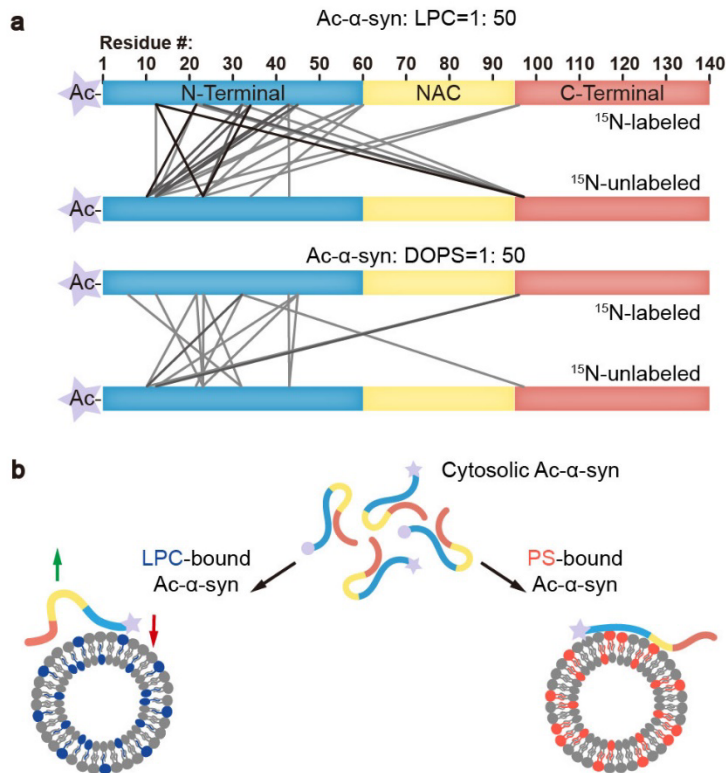
Figure 4 Ac-α-syn binding on LPC shows high intermolecular interactions. (**a**) The cross-linking patterns of Ac-α-syn in the presence of LPC and DOPS mapped by MS at the protein/lipid molar ratio of 1:50. Lines present the inter-molecular cross-linked residues between two individual ^{15}N-labeled and unlabeled Ac-α-syn. The grayscale of the lines corresponds to the frequency of the cross-linked pairs identified in three individual experiments. Source data are provided in **Tables S1-S6**. (**b**) Ac-α-syn binds strongly to LPC through the N-terminal region (red arrow), and leaves more unbound NAC and C-terminal region for intermolecular interaction (green arrow). In contrast, N-terminal acetylation reduces α-syn's binding to DOPS, and due to the negatively charged headgroup of PS, Ac-α-syn binding on DOPS extends to the NAC region, which limits intermolecular interactions.

References:

1. Diao, J., Burre, J., Vivona, S., Cipriano, D.J., Sharma, M., Kyoung, M., Sudhof, T.C., and Brunger, A.T. (2013). Native alpha-synuclein induces clustering of synaptic-vesicle mimics via binding to phospholipids and synaptobrevin-2/VAMP2. Elife *2*, e00592. 10.7554/eLife.00592.

2. Lai, Y., Zhao, C., Tian, Z., Wang, C., Fan, J., Hu, X., Tu, J., Li, T., Leitz, J., Pfuetzner, R.A., et al. (2023). Neutral lysophosphatidylcholine mediates α-synuclein-induced synaptic vesicle clustering. Proc Natl Acad Sci U S A *120*, e2310174120. 10.1073/pnas.2310174120.

3. Burre, J., Sharma, M., Tsetsenis, T., Buchman, V., Etherton, M.R., and Sudhof, T.C. (2010). alpha-Synuclein Promotes SNARE-Complex Assembly in Vivo and in Vitro. Science *329*, 1663-1667. Doi 10.1126/Science.1195227.

4. Wang, C., Zhang, K., Cai, B., Haller, J.E., Carnazza, K.E., Hu, J., Zhao, C., Tian, Z., Hu, X., Hall, D., et al. (2024). VAMP2 chaperones α-synuclein in synaptic vesicle co-condensates. Nat Cell Biol *26*, 1287-1295. 10.1038/s41556-024-01456-1.

5. Goedert, M., Spillantini, M.G., Del Tredici, K., and Braak, H. (2013). 100 years of Lewy pathology. Nat Rev Neurol *9*, 13-24. 10.1038/nrneurol.2012.242.

6. Uversky, V.N., and Eliezer, D. (2009). Biophysics of Parkinson's disease: structure and aggregation of alpha-synuclein. Curr Protein Pept Sci *10*, 483-499. 10.2174/138920309789351921.

7. Li, D., and Liu, C. (2022). Conformational strains of pathogenic amyloid proteins in neurodegenerative diseases. Nat Rev Neurosci *23*, 523-534. 10.1038/s41583-022-00603-7.

8. Fauvet, B., Fares, M.B., Samuel, F., Dikiy, I., Tandon, A., Eliezer, D., and Lashuel, H.A. (2012). Characterization of semisynthetic and naturally Nα-acetylated α-synuclein in vitro and in intact cells: implications for aggregation and cellular properties of α-synuclein. J Biol Chem *287*, 28243-28262. 10.1074/jbc.M112.383711.

9. Oueslati, A. (2016). Implication of Alpha-Synuclein Phosphorylation at S129 in Synucleinopathies: What Have We Learned in the Last Decade? J Parkinsons Dis *6*, 39-51. 10.3233/jpd-160779.

10. Mahul-Mellier, A.L., Fauvet, B., Gysbers, A., Dikiy, I., Oueslati, A., Georgeon, S., Lamontanara, A.J., Bisquertt, A., Eliezer, D., Masliah, E., et al. (2014). c-Abl phosphorylates α-synuclein and regulates its degradation: implication for α-synuclein clearance and contribution to the pathogenesis of Parkinson's disease. Hum Mol Genet *23*, 2858-2879. 10.1093/hmg/ddt674.

11. Zhang, H., Zhu, L., Sun, L., Zhi, Y., Ding, J., Yuan, Y.S., Shen, F.F., Li, X., Ji, P., Wang, Z., et al. (2019). Phosphorylated α-synuclein deposits in sural nerve deriving from Schwann cells: A biomarker for Parkinson's disease. Parkinsonism Relat Disord *60*, 57-63. 10.1016/j.parkreldis.2018.10.003.

12. Hu, J., Xia, W., Zeng, S., Lim, Y.J., Tao, Y., Sun, Y., Zhao, L., Wang, H., Le, W., Li, D., et al. (2024). Phosphorylation and O-GlcNAcylation at the same α-synuclein site generate distinct fibril structures. Nat Commun *15*, 2677. 10.1038/s41467-024-46898-1.

13. Theillet, F.X., Binolfi, A., Bekei, B., Martorana, A., Rose, H.M., Stuiver, M., Verzini, S., Lorenz, D., van Rossum, M., Goldfarb, D., and Selenko, P. (2016). Structural disorder of monomeric alpha-synuclein persists in mammalian cells. Nature *530*, 45-50. 10.1038/nature16531.

14. Marotta, N.P., Lin, Y.H., Lewis, Y.E., Ambroso, M.R., Zaro, B.W., Roth, M.T., Arnold, D.B., Langen, R., and Pratt, M.R. (2015). O-GlcNAc modification blocks the aggregation and toxicity of the protein α-synuclein associated with Parkinson's disease. Nat Chem *7*, 913-920. 10.1038/nchem.2361.

15. Li, X., Pinou, L., Du, Y., Chen, X., and Liu, C. (2023). Emerging roles of O-glycosylation in regulating protein aggregation, phase separation, and functions. Curr Opin Chem Biol *75*, 102314. 10.1016/j.cbpa.2023.102314.

16. Bu, B., Tong, X., Li, D., Hu, Y., He, W., Zhao, C., Hu, R., Li, X., Shao, Y., Liu, C., et al. (2017). N-Terminal Acetylation Preserves alpha-Synuclein from Oligomerization by Blocking Intermolecular Hydrogen Bonds. ACS Chem Neurosci *8*, 2145-2151. 10.1021/acschemneuro.7b00250.

17. Runfola, M., De Simone, A., Vendruscolo, M., Dobson, C.M., and Fusco, G. (2020). The N-terminal Acetylation of α-Synuclein Changes the Affinity for Lipid Membranes but not the Structural Properties of the Bound State. Sci Rep *10*, 204. 10.1038/s41598-019-57023-4.

18. Trexler, A.J., and Rhoades, E. (2012). N-Terminal acetylation is critical for forming α-helical oligomer of α-synuclein. Protein Sci: a publication of the Protein Society *21*, 601-605. 10.1002/pro.2056.

19. Fusco, G., Pape, T., Stephens, A.D., Mahou, P., Costa, A.R., Kaminski, C.F., Kaminski Schierle, G.S., Vendruscolo, M., Veglia, G., Dobson, C.M., and De Simone, A. (2016). Structural basis of synaptic vesicle assembly promoted by alpha-synuclein. Nat Commun *7*, 12563. 10.1038/ncomms12563.

20. Wang, C., Tu, J., Zhang, S., Cai, B., Liu, Z., Hou, S., Zhong, Q., Hu, X., Liu, W., Li, G., et al. (2020). Different regions of synaptic vesicle membrane regulate VAMP2 conformation for the SNARE assembly. Nat Commun *11*, 1531. 10.1038/s41467-020-15270-4.

21. Wilhelm, B.G., Mandad, S., Truckenbrodt, S., Kröhnert, K., Schäfer, C., Rammner, B., Koo, S.J., Claßen, G.A., Krauss, M., Haucke, V., et al. (2014). Composition of isolated synaptic boutons reveals the amounts of vesicle trafficking proteins. Science *344*, 1023-1028. 10.1126/science.1252884.

22. Burré, J., Sharma, M., and Südhof, T.C. (2018). Cell Biology and Pathophysiology of α-Synuclein. Cold Spring Harb Perspect Med *8*. 10.1101/cshperspect.a024091.

23. Anderson, J.P., Walker, D.E., Goldstein, J.M., de Laat, R., Banducci, K., Caccavello, R.J., Barbour, R., Huang, J., Kling, K., Lee, M., et al. (2006). Phosphorylation of Ser-129 is the dominant pathological modification of alpha-synuclein in familial and sporadic Lewy body disease. J Biol Chem *281*, 29739-29752. 10.1074/jbc.M600933200.

24. Lauwers, E., Goodchild, R., and Verstreken, P. (2016). Membrane Lipids in Presynaptic Function and Disease. Neuron *90*, 11-25. 10.1016/j.neuron.2016.02.033.

25. Zhao, C., Tu, J., Wang, C., Liu, W., Gu, J., Yin, Y., Zhang, S., Li, D., Diao, J., Zhu, Z.J., and Liu, C. (2024). Lysophosphatidylcholine binds α-synuclein and prevents its pathological aggregation. Natl Sci Rev *11*, nwae182. 10.1093/nsr/nwae182.

26. Emre, C., Do, K.V., Jun, B., Hjorth, E., Alcalde, S.G., Kautzmann, M.I., Gordon, W.C., Nilsson, P., Bazan, N.G., and Schultzberg, M. (2021). Age-related changes in brain phospholipids and bioactive lipids in the APP knock-in mouse model of Alzheimer's disease. Acta Neuropathol Commun *9*, 116. 10.1186/s40478-021-01216-4.

27. Johnson, M., Coulton, A.T., Geeves, M.A., and Mulvihill, D.P. (2010). Targeted amino-terminal acetylation of recombinant proteins in E. coli. Plos One *5*, e15801. 10.1371/journal.pone.0015801.

28. Ahmed, S., Holt, M., Riedel, D., and Jahn, R. (2013). Small-scale isolation of synaptic vesicles from mammalian brain. Nat Protoc *8*, 998-1009. 10.1038/nprot.2013.053.

29. Diao, J., Ishitsuka, Y., Lee, H., Joo, C., Su, Z.L., Syed, S., Shin, Y.K., Yoon, T.Y., and Ha, T. (2012). A single vesicle-vesicle fusion assay for in vitro studies of SNAREs and accessory proteins. Nat Protoc *7*, 921-934. Doi 10.1038/Nprot.2012.020.

30. Schanda, P., and Brutscher, B. (2005). Very fast two-dimensional NMR spectroscopy for real-time investigation of dynamic events in proteins on the time scale of seconds. J Am Chem Soc *127*, 8014-8015. 10.1021/ja051306e.

31. Schanda, P., Kupce, E., and Brutscher, B. (2005). SOFAST-HMQC experiments for recording two-dimensional heteronuclear correlation spectra of proteins within a few seconds. J Biomol NMR *33*, 199-211. 10.1007/s10858-005-4425-x.

32. Takamori, S., Holt, M., Stenius, K., Lemke, E.A., Gronborg, M., Riedel, D., Urlaub, H., Schenck, S., Brugger, B., Ringler, P., et al. (2006). Molecular anatomy of a trafficking organelle. Cell *127*, 831-846. Doi 10.1016/J.Cell.2006.10.030.

33. Delaglio, F., Grzesiek, S., Vuister, G.W., Zhu, G., Pfeifer, J., and Bax, A. (1995). NMRPipe: a multidimensional spectral processing system based on UNIX pipes. J Biomol NMR *6*, 277-293. 10.1007/bf00197809.

34. Bermel, W., Bertini, I., Felli, I.C., Lee, Y.M., Luchinat, C., and Pierattelli, R. (2006). Protonless NMR experiments for sequence-specific assignment of backbone nuclei in unfolded proteins. J Am Chem Soc *128*, 3918-3919. 10.1021/ja0582206.

35. Fan, S.B., Meng, J.M., Lu, S., Zhang, K., Yang, H., Chi, H., Sun, R.X., Dong, M.Q., and He, S.M. (2015). Using pLink to Analyze Cross-Linked Peptides. Curr Protoc Bioinformatics *49*, 8.21.21-28.21.19. 10.1002/0471250953.bi0821s49.